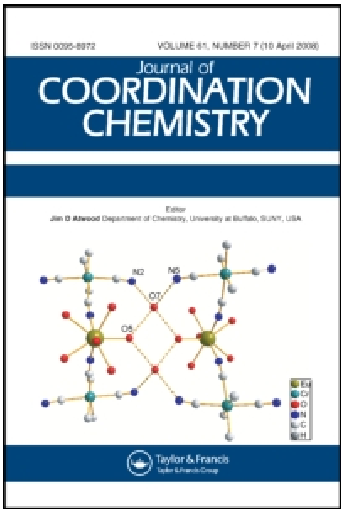

Journal of Coordination Chemistry
Publication details, including instructions for authors and subscription information:
http://www.informaworld.com/smpp/title~content=t713455674

Ligating Properties of 5-Nitrobarbituric Acid

M. S. Masoud[a]; A. KH. Ghonam[a]; R. H. Ahmed[a]; S. A. Aboud El-Enein[a]; A. A. Mahmoud[a]
[a] Chemistry Department, Faculty of Science, Alexandria University, Egypt

Online publication date: 15 September 2010

To cite this Article Masoud, M. S. , Ghonam, A. KH. , Ahmed, R. H. , El-Enein, S. A. Aboud and Mahmoud, A. A.(2002) 'Ligating Properties of 5-Nitrobarbituric Acid', Journal of Coordination Chemistry, 55: 1, 79 — 105
To link to this Article: DOI: 10.1080/00958970211870
URL: http://dx.doi.org/10.1080/00958970211870

J. Coord. Chem., 2002, Vol. 55(1), pp. 79 – 105

LIGATING PROPERTIES OF 5-NITROBARBITURIC ACID

M. S. MASOUD[a,*], A. KH. GHONAIM[b], R. H. AHMED[a], S. A. ABOU EL-ENEIN[c] and A. A. MAHMOUD[a]

[a]*Chemistry Department, Faculty of Science, Alexandria University, Egypt;*
[b]*Chemistry Department, Faculty of Science, Zagazig University, Egypt;*
[c]*Chemistry Department, Faculty of Science, Menofia University, Shebin El Kome, Egypt*

(Received 2 June 2000; In final form 10 October 2000)

The dissociation constant of 5-nitrobarbituric acid and the stability constants of its Co^{II}, Ni^{II} and Cu^{II} complexes were determined potentiometrically. The thermodynamic parameters of dissociation were evaluated. The effect of solvents on the pK values was explained from aquation and solvation views. 5-Nitrobarbituric acid solid complexes of Mn^{II}, Co^{II}, Ni^{II}, Cu^{II} and Zn^{II}, and the mixed metals, Fe–Co, Fe–Ni were prepared and characterized based on elemental analysis, spectra (electronic, IR, and Mössbauer), magnetism and thermal measurements.

Keywords: 5-Nitrobarbituric acid; Co(II); Ni(II); Cu(II)

INTRODUCTION

N-Heterocyclic compounds containing amide linkages are widely used in medicine, *e.g.*, as hypnotic drugs, and produce depressive effects on the central nervous system [1]. Most pyrimidines have antimicrobial, anti-inflammatory and antitumor properties [2, 3]. Masoud *et al.* [4 – 44] published a series of papers on the chemistry of pyrimidine compounds and their complexes. 5-Nitrobarbituric acid (I) forms the

*Corresponding author. Fax: 002 03 4911794, e-mail: drmsmasoud@yahoo.com

ISSN: 0095-8972 DOI: 10.1080/00958970290000669

basis of this paper.

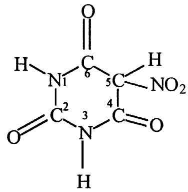

(I)

5-Nitrobarbituric acid was reported for the identification of 4-amino-pyridine by microcrystal reaction [45]. Some drugs containing amino groups were identified by studying their microcrystal structures after reaction with 5-nitrobarbituric acid [46, 47]. Nucleobase analogues were screened as inhibitors of dihydrouracil dehydrogenase from mouse liver [48]. 5-Nitrobarbituric acid was identified as a potent inhibitor of this activity [49 – 52]. Liquid membrane electrode systems responsive to the nicotinium cation were described on the use of the ion-association complexes of cation were nicotinium cation with 5-nitrobarbiturate counter anions in nitrobenzene solvent as ion-exchange sites [53]. The performance characteristics of these electrodes with high sensitivity and fast response for the nicotinium cation were evaluated and used satisfactorily for the direct determination of nicotine in tobacco smoke [53]. Polyvinyl chloride matrix membrane buformin-selective electrodes have been developed for the direct determination of the buformin cation in aqueous solutions [54]. These membrane electrodes were based on the use of ion-association complexes of the buformin hydrochloride cation with 5-nitrobarbiturates counter ions as ion-exchange sites. 5-Nitrobarbituric acid ligand was found to form monoclinic complexes with alkali, alkaline and rare earth metals [55, 56]. The complexes were characterized by IR spectra, thermal decomposition and solubility studies [57].

The purposes of this manuscript are: (i) evaluation of both the acid dissociation constant in 25 – 75%(v/v) ethanol-water and dioxane-water mixtures at different temperatures (25 – 45°C) and the stability constants of the complexes using potentiometric techniques, and (ii) structural determination of the prepared simple and mixed metal complexes from IR, UV, magnetic susceptibility, Mössbauer spectra and thermal analysis techniques.

EXPERIMENTAL

30 mmol of 5-nitrobarbituric acid was dissolved in dioxane by heating, then mixed with an alcoholic solution of 10 – 20 mmol of the iron(III) chloride

and the reaction mixture was refluxed for 1 hr at 70°C. The mixture was cooled with a complex precipitated, separated by filtration, washed with hot dioxane and dried in a vacuum desiccator over P_2O_5.

An ammoniacal solution of 0.01 mol of the metal(II) chloride [manganese(II), cobalt(II), nickel(II), copper(II) or zinc(II)] was mixed with an ammoniacal solution of 0.01 mol of 5-nitrobarbituric acid. The reaction mixture was refluxed for 2–3 hours at 70°C, then left overnight for precipitation. The complexes were separated by filtration, washed by ethanol and dried in a desiccator over anhydrous $CaCl_2$. The mixed metal complexes were prepared similarly to the simple complexes. The mole ratio of the ligand to both metal salts (Co^{II}, Ni^{II}, Fe^{III}) was 1 : 1 : 1. The reaction mixture was cooled, separated by filtration and dried in vacuum desiccator over P_2O_5. The stoichiometry of all the complexes was determined as usual. The analytical data are collected in Table I.

The pH meter used was a Cole-Parmer Model 60648 pH. The electrode system was calibrated before and after each series of pH measurements under the same conditions using standard buffers pH's 4.0 and 7.0. The titration cell consisted of a 150 mL water-jacketed vessel fit with a polyethylene stopper in which appropriately located holes are present, one of them allowed the insertion of a 4 ml microburette accurate to 0.02 mL. The burette was filled by gentle suction exerted by a water pump and the KOH was protected from the atmospheric CO_2 by a tube containing $CaCl_2$. Another hole was used to insert the combined electrode. The titrations were recorded in presence of purified nitrogen gas. The potentiometric titration procedure was applied to evaluate the dissociation constants of the organic compounds by introducing the appropriate volume of the organic compound into the titration cell in presence of 5 mL of 0.5 M KCl solution and 25%, 35%, 50% and 75%(v/v) ethanol-water and dioxane-water. The solution in the titration vessel was left for about 15 min to attain the desired temperature control by using a thermostatic Techne model U10. During the whole titration, purified nitrogen gas was slowly bubbled in the solution. The same potentiometric titration experiment was used for studying the complex equilibria in 75%(v/v) ethanol-water as follow: The complex solution (1 mL 10^{-3} M metal ion + 5 mL 10^{-3} M ligand + 5 mL 0.5 M KCl + 32.5 mL ethanol and completed to 50 mL by distilled water) was titrated against standard KOH. The experiment was done under the same conditions as for titrating the organic compound against standard KOH (at controlled ionic strength and constant temperature). The pH-meter readings (B) recorded in 75%(v/v) ethanol-water and dioxane-water solutions were converted to hydrogen ion concentration $[H^+]$ by means of the relation of

TABLE I Colors, analysis, nujol mull electronic spectra and magnetic moments of the complexes

Complex	Color	%calculated (%found) M	N	Cl	μ_{eff} at 298° K	$\lambda_{max}(cm^{-1})$
(a) Simple complexes						
$MnL_2 \cdot 6H_2O$	Buff	10.79 (10.76)	16.50 (16.10)	– –	5.88	40820, 33840, 31110, 27917, 17920
$FeLCl \cdot 3H_2O$	Pale brown	15.80 (15.60)	11.47 (12.10)	19.94 (20.05)	6.1	38869, 28469, 21276, 16130
$CoL_3 \cdot 2H_2O$	Pale violet	9.56 (9.52)	20.50 (20.42)	– –	5.8	42796, 33222, 20000
$NiL_3 \cdot 5H_2O$	Bluish-green	8.79 (8.89)	18.90 (19.10)	– –	3.4	41666, 31305, 25000, 18050
$CuL_3 \cdot H_2O$	Pale green	10.56 (10.42)	20.90 (20.70)	– –	2.3	40650, 31250, 18870
$ZnL_4 \cdot H_2O$	White	8.23 (8.19)	21.17 (21.07)	– –	–	–

Complex	Color	%calculated (%found) Fe	Co	Ni	N	Cl	μ_{eff} at 298° K	$\lambda_{max}(cm^{-1})$
(b) Mixed complexes								
$Ni_3FeL_7Cl_2 \cdot H_2O$	Pale yellow	3.64 (3.90)	– –	11.50 (11.04)	19.20 (20.10)	4.60 (3.90)	5.78	39841, 34483, 21053, 18149
$Co_3FeL_7Cl_2 \cdot H_2O$	Yellow	3.60 (3.72)	11.50 (11.40)	– –	19.18 (19.80)	4.63 (3.70)	9.1	30581, 17690

Van Uitert and Haas [58]:

$$-\log[H^+] = B + \log U_H^\circ - \log 1/\nu^2$$

ν is the activity coefficient of the solvent composition and ionic strength for which U_H° was determined.
B is the pH-meter reading.
U_H° is the correction factor at zero ionic strength for the solvent composition under investigation ($U_H^\circ = 0.26$).

Electronic absorption spectra were made with a Pye–Unicam SP1800 spectrophotometer.

The KBr disk infrared spectra were recorded using a Pye–Unicam SP1025 and SP3-100 spectrophotometer equipped with NaCl prism over the frequency range 200–4000 cm^{-1}.

Molar magnetic susceptibilities, corrected for diamagnetism using Pascal's constants, were determined at room temperature (298°K) using Faraday's method. The apparatus was calibrated with $Hg[Co(SCN)_4]$ [59].

Mössbauer spectra were recorded at room temperature using a computerized Ranger Ms-1200 in standard transmission geometry with a 20 m Ci Co [57] (Rh) source. The data have been analyzed by means of least square computer fitting using the Mossfit computer program. The isomer shift values refer to that of metallic iron at room temperature.

Thermogravimetric measurements were preformed on a DU Pont 9900 computerized thermal analyzer. The heating rate was 10 degree/min. 60 mg of the sample was placed in a platinum crucible. Dry nitrogen was passed over the sample at a rate of 10 cc/min and a chamber cooling water flow rate was 101/h. The speed was 5 mm/min.

RESULTS AND DISCUSSION

Potentiometric Studies

The potentiometric studies of 5-nitrobarbituric acid in aqueous media were done in ethanol-water and dioxane-water media at different temperatures (25–45°C). The experiments for the complex solutions were done in aqueous media. Acidity and stability constants were determined by using acid–base titration techniques. The application of the potentiometric measurements depends on evaluation of the average number of the protons associated with the reagent $\bar{n}_A^{56}$, based on the following equation [5, 60]:

$$\bar{n}_A = Y - \frac{V_i N^0}{V_0 C_L^\circ}$$

V_1 is the volume of alkali required to reach a given pH on the titration curve; V_0 is the initial volume of the ligand; N^0 is the alkali concentration; C_L° is the total concentration of the ligand and Y is the number of displaceable hydrogen atoms in the ligand. The dissociation constants were obtained by plotting $\bar{n}_A$ against pH for the free ligand. Two pK values were evaluated with $Y = 2$ by recording the pH values at $\bar{n}_A = 0.5$ and 1.5. The point-wise calculation procedure [61] was used for the same purpose, where concordant results are obtained, Table II, based on the following equations where the ligand is symbolized as H_3L:

$$pH = \log \frac{\bar{n}_A - 2}{3 - \bar{n}_A} + pK_1$$

$$pH = \log \frac{\bar{n}_A - 1}{2 - \bar{n}_A} + pK_2$$

The plot of the $\log \bar{n}_A$ ratio *vs.* pH gives the required pK values. A basic method of calculation constructed by Martell [62] was applied to calculate the acid dissociation constants, Table II, where the equilibria involved are as follows:

$$H_3A \rightleftharpoons H^+ + H_2A^- \quad K_1 = [H^+][H_2A^-]/[H_3A]$$

$$H_2A^- \rightleftharpoons H^+ + HA^{2-} \quad K_2 = [H^+][HA^{-2}]/[H_2A^-]$$

Since $K_1 > K_2$ each dissociation stage was considered separately. If C_A represents the total concentration of the ligand species and "a" represents the number of moles of base added per mole of ligand, it follows that in the low pH buffer region:

$$C_A = [H_3A] + [H_2A^-] + [HA^{2-}]$$

$$aC_A + [H^+] = [H_2A^-] + 2[HA^{2-}]$$

The first dissociation constant is calculated from the following equation:

$$K_1 = \frac{[H^+](aC_A + [H^+] - [HA^{2-}])}{C_A - (aC_A + [H^+])}$$

TABLE II pK values for 5-nitrobarbituric acid in ethanol-water media at different temperatures and dioxane-water media at 25°C

	Point-wise method					*Algebraic method*				
% of solvent	25°*C*	30°*C*	35°*C*	40°*C*	45°*C*	25°*C*	30°*C*	35°*C*	40°*C*	45°*C*
Aqueous media	3.59 (9.96)	3.67 (9.86)	3.73 (9.70)	3.84 (9.70)	3.92 (9.66)	3.07 (10.12)	3.27 (10.01)	3.38 (9.85)	3.58 (9.80)	3.72 (9.74)
25%(v/v) ethanol-water	4.21 (10.73)	4.30 (10.61)	4.40 (10.50)	4.50 (10.41)	4.60 (10.30)	4.10 (11.06)	4.22 (10.87)	4.33 (10.72)	4.46 (10.58)	4.56 (10.44)
35%(v/v) ethanol-water	3.36 (10.81)	4.56 (10.74)	4.69 (10.62)	4.80 (10.53)	5.00 (10.44)	4.31 (11.12)	4.44 (10.97)	4.68 (10.75)	4.86 (10.67)	5.02 (10.55)
50%(v/v) ethanol-water	6.41 (11.28)	6.52 (11.17)	6.63 (11.08)	6.75 (10.98)	6.88 (10.89)	6.44 (11.68)	6.52 (11.46)	6.64 (11.32)	6.77 (11.17)	6.89 (11.05)
75%(v/v) ethanol-water	7.42 (11.75)	7.52 (11.63)	7.63 (11.54)	7.76 (11.43)	7.85 (11.31)	7.51 (11.85)	7.60 (11.69)	7.71 (11.60)	7.53 (11.47)	7.92 (11.34)
25%(v/v) dioxane-water	4.27 (10.12)	4.01 (10.05)	3.88 (9.95)	3.70 (9.75)	–	4.20 (10.19)	38.4 (10.10)	3.69 (10.02)	3.36 (9.78)	–
35%(v/v) dioxane-water	3.98 (10.53)	–	–	–	–	3.65 (10.58)	–	–	–	–
50%(v/v) dioxane-water	4.18 (11.09)	–	–	–	–	4.04 (11.11)	–	–	–	–
75%(v/v) dioxane-water	5.48 (12.33)	–	–	–	–	5.50 (12.34)	–	–	–	–

Values in parentheses are pk_2 values.

In the high pH buffer region the C_A value is as follows:

$$C_A = [H_2A^-] + [HA^{2-}] + [A^{3-}]$$
$$(a-1)C_A - [OH^-] = [A^{3-}]$$

Under these conditions, K_2 is expressed by:

$$K_2 = \frac{[H^+][HA^{2-}]}{C_A - [HA^{2-}] + ((a-1)C_A - [OH^-])}$$

The pK values of 5-nitrobarbituric acid are increased with increasing percentage of ethanol in an ethanol-water mixture and with increasing the percentage of dioxane in a dioxane-water mixture. 5-Nitrobarbituric acid gave two pK values in different percentages of ethanol-water and dioxane-water (25%, 35%, 50% and 75%) at different temperatures (25–45°C). The $\Delta G°$, $\Delta H°$ and $\Delta S°$ values are evaluated and collected in Table III. The familiar equation: $K = A\,e^{-\Delta E/RT}$ is applied for studying the effect of temperature on the pK values. On plotting the pK values *vs.* 1/T, straight lines are obtained with a slope of $\Delta H°/2.3R$ from which the $\Delta H°$ values ($Kcal\,mol^{-1}$) are computed. The free energy $\Delta G°$ ($kcal\,mol^{-1}$) values are given using the equation $\Delta G° = 2.3RT$ pK. The $\Delta S°$ (e.u.) values are calculated using the relation $\Delta G° = \Delta H° - T\Delta S°$. The pK values of 5-nitrobarbituric acid are increased with increasing temperature. The values of $\Delta H°$ based on the pK_1 values are negative while those based on pK_2 values are independent on the percentages of ethanol-water mixture, $-\Delta S°$ values for 5-nitrobarbituric acid in different percentages of ethanol-water mixture are attributed to the presence of intermolecular hydrogen bonding [63]. The effects of ethanol and dioxane solvents on 5-nitrobarbituric acid is considered as follows: If the J factor represents solvent-transfer where the following relation is tested [64]:

$$J\log[S] - \log K = -\Delta G°/(2.303RT) - W\log[H_2O]/[S] + J\log[H_2O],$$
$$\text{where:}\quad \log[H_2O]/[S] = X;\ J\log[S] - \log K = Y$$

[S] and $\Delta G°$ represent the solvent concentration and the free energy, respectively. The data are collected in Table IV. Y is plotted against X, a representative example is given in Figure 1. Trail values of J = 1, 2, 3, 4 are used to find values of (W) for the gradient of Y *vs.* X. The slopes of the X–Y relation gave values for water molecules (W). The data obtained may throw light on the role of aquation and solvation during the course of

TABLE III Thermodynamic parameters of ionization of 5-nitrobarbituric acid in different percentages of ethanol-water

	pK					$\Delta G^\circ_{25^\circ C}$ *kcal*	ΔH° *kcal*	ΔS°
% of ethanol-water	$25^\circ C$	$30^\circ C$	$35^\circ C$	$40^\circ C$	$45^\circ C$	$mol^{-1}K^{-1}$	$mol^{-1}K^{-1}$	*e.u.*
Aqueous media	3.59 (9.96)	3.67 (9.88)	3.75 (9.78)	3.85 (9.71)	3.93 (9.65)	4.92 (13.65)	−7.53 (7.11)	−41.77 (−21.96)
25% ethanol-water	4.21 (10.73)	4.32 (10.61)	4.42 (10.51)	4.52 (10.41)	4.62 (10.30)	5.77 (14.71)	−8.36 (8.36)	−47.43 (−21.29)
35% etanol-water	4.36 (10.83)	4.54 (10.73)	4.70 (10.63)	4.84 (10.54)	5.00 (10.54)	5.98 (14.85)	−2.55 (7.95)	−62.15 (−23.16)
50% ethanol-water	6.42 (11.29)	6.52 (11.17)	6.63 (11.08)	6.75 (10.98)	6.86 (10.89)	8.80 (15.48)	−9.20 (7.95)	−60.40 (−25.27)
75% ethanol-water	7.42 (11.76)	7.54 (11.63)	7.63 (11.54)	7.74 (11.43)	7.84 (11.31)	10.17 (16.12)	−8.36 (9.2)	−62.20 (−23.22)

TABLE IV X−Y date of 5-nitrobarbituric acid in different percentages of ethanol-water media at different temperatures and dioxane-water media at 25°C*

[s]%	− log[s]	− X	J = 1	J = 2	J = 3	J = 4	J = 1	J = 2	J = 3	J = 4	J = 1	J = 2	J = 3	J = 4
				Y, 25°C				Y, 30°C				Y, 35°C		
25	0.6021	−0.477	3.61 (10.13)	3.01 (9.53)	2.40 (8.92)	1.80 (8.32)	3.72 (10.01)	3.12 (9.41)	2.51 (8.80)	1.91 (8.20)	3.82 (9.91)	3.22 (9.31)	2.61 (8.70)	2.01 (8.10)
35	0.4559	−0.269	3.9 (10.37)	4.45 (9.92)	2.99 (9.46)	2.54 (9.01)	4.08 (10.27)	3.63 (9.82)	3.17 (9.36)	2.72 (8.91)	4.24 (10.17)	3.79 (9.72)	3.33 (9.26)	2.88 (8.81)
50	0.301	Zero	6.12 (10.99)	5.82 (10.69)	5.52 (10.39)	2.22 (10.09)	6.22 (10.87)	5.92 (10.57)	5.62 (10.27)	5.32 (9.97)	6.33 (10.78)	6.03 (10.48)	5.73 (10.18)	5.43 (9.88)
75	0.1249	0.477	7.3 (11.64)	7.17 (11.51)	7.05 (11.39)	6.92 (11.26)	7.42 (11.51)	7.29 (11.38)	7.17 (11.26)	7.04 (11.13)	7.51 (11.42)	7.38 (11.29)	7.20 (11.17)	7.13 (11.04)
				Y, 40°C				Y, 45°C				Y, 25°C*		
25	0.6021	−0.477	3.92 (9.81)	3.32 (9.12)	2.71 (8.60)	2.11 (8.00)	4.02 (9.70)	3.42 (9.10)	2.80 (8.49)	2.21 (7.89)	3.28 (9.53)	2.68 (8.93)	2.07 (8.32)	1.47 (7.72)
35	0.4559	−0.269	4.38 (10.08)	3.93 (9.63)	3.47 (9.17)	3.02 (8.72)	4.54 (9.99)	4.09 (9.54)	3.63 (9.08)	3.18 (8.63)	3.54 (10.07)	3.09 (9.62)	2.63 (9.16)	2.18 (8.71)
50	0.301	Zero	6.45 (10.68)	6.15 (10.38)	5.85 (10.08)	5.55 (9.78)	6.50 (10.59)	6.26 (10.29)	5.96 (9.99)	5.66 (9.69)	3.88 (10.79)	3.58 (10.49)	3.28 (10.19)	2.98 (9.89)
75	0.1249	0.477	7.62 (11.31)	7.49 (11.18)	7.37 (11.06)	7.24 (10.93)	7.72 (11.19)	7.59 (11.06)	7.47 (10.94)	7.34 (10.81)	4.36 (12.21)	4.23 (12.08)	4.11 (11.96)	3.98 (11.83)

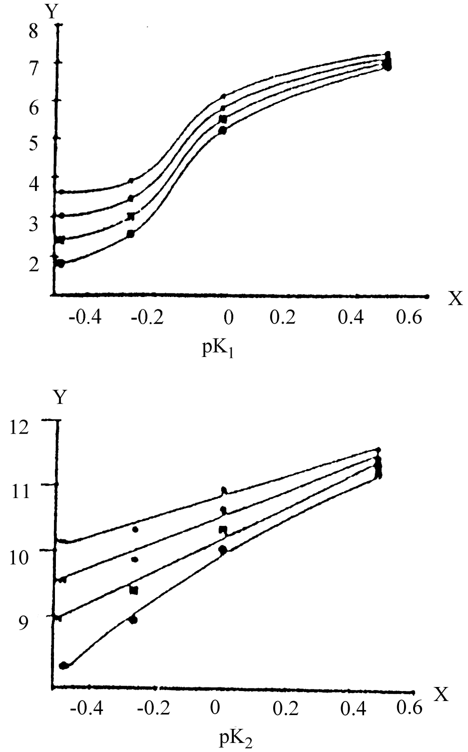

FIGURE 1 X–Y relationship for pK_1 and pK_2 of 5-nitrobarbituric acid in different percentages of ethanol-water at 25°C.

dissociation. For 5-nitrobarbituric acid in different percentages of ethanol-water mixtures, the calculated (W) values are higher than that of J($J = 1, 2$) at temperatures from 25–45°C point to more aquation. By increasing the temperature, the values of (W) are smaller than that of J (for $J = 3$ and 4) which suggests more solvation. In the temperature range 25–45°C the values of (W) for different values of J are independent of temperature. In different percentages of dioxane-water mixtures at 25°C it is obvious that, the values of (W) for different values of J calculated based on pK_2 values are greater than the values of J which suggests more aquation.

The acid–base properties of the free ligand facilitate investigation of its coordinating behavior towards Co^{II}, Ni^{II} and Cu^{II}. The complex solutions [1M: 1L] are titrated against standard KOH in presence of 0.5 M KCl solution as a supporting electrolyte at 25°C. The measurements could be used to calculate the free ligand exponent pL, the degree of formation of the system n and hence the stability constants of the metal-ligand complexes present. The metal-ligand formation number $\bar{n}$ is defined as:

$$\bar{n} = \frac{C_L - (C_H + [H^+]/\bar{n}_A)}{C_M}$$

where C_L and C_M are the analytical concentrations of ligand and metal, respectively. Plotting $\bar{n}$ *vs.* pL at $\bar{n}$ equal to 0.5 and 1.5 where $\log K_1$ and $\log K_2$ values are calculated, respectively, Figures 2a–c, concordant results are obtained on applying the pointwise calculation method [60] where:

$$\log K_1 = pL + \log \frac{\bar{n}}{1 - \bar{n}} \qquad \bar{n} < 1$$

$$\log K_2 = pL + \log \frac{2 - \bar{n}}{\bar{n} - 1} \qquad 1 < \bar{n} < 2$$

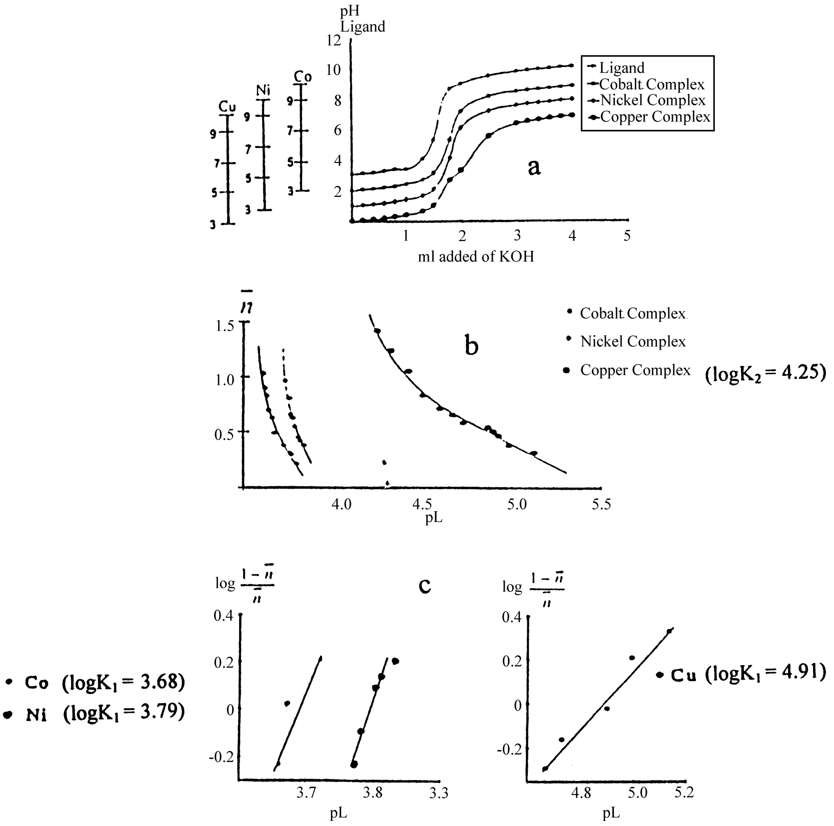

FIGURE 2 (a) pH-titration of 5-nitrobarbituric acid and its complexes $[L] = 1 \times 10^{-3}$ M, $[M] = 1 \times 10^{-4}$ M in aqueous media at 25°C. (b) $\bar{n}$ – pL relationship of 5-nitrobarbituric acid complexes in aqueous media at 25°C. (c) Point-wise plots of 5-nitrobarbituric acid complexes in aqueous media at 25°C.

On plotting $\log \bar{n}$ function *vs.* pL, straight lines are obtained from which the respective log K values are computed.

Studies on the Solid Complexes

Infrared Spectra

(1) The strong broad ν_{OH} band at 3399 cm^{-1} in the free ligand moves to 3369, 3423, 3437, 3438, 3462 and 3553 cm^{-1} for Mn^{II}, Fe^{III}, Co^{II}, Ni^{II}, Cu^{II} and Zn^{II} complexes, respectively.
(2) The strong ν_{NH} band at 3170–3000 cm^{-1} in the spectra of all complexes indicated that only one of the two (N–H) groups is involved in coordination.
(3) The medium ν_{CH} band at 2831 cm^{-1} for the free ligand is slightly affected ($\pm$5 cm^{-1}) on complexation. New bands at 2695, 2694 and 2692 cm^{-1} for Co^{II}, Ni^{II} and Mn^{II} complexes are due to hydrogen bonded or aquo structures.
(4) The medium $\nu_{C{=}N}$ in the free ligand assigned at 1639 cm^{-1} is due to tautomerism. The Mn^{II} complex gave three $\nu_{C{=}N}$ bands at 1691, 1660 and 1615 cm^{-1}. For Fe^{III}, Ni^{II} and Zn^{II} complexes, the $\nu_{C{=}N}$ moved to 1646, 1617 and 1644 cm^{-1}, respectively. However, the Co^{II} complex gave two bands at 1661 and 1616 cm^{-1}. Such data suggest that the nitrogen atom of the pyrimidine ring formed by tautomerism is bonded to the metal.
(5) For the nitro group, the free ligand showed two bands at 1480 and 1383 cm^{-1} due to $\nu_{asym}NO_2$ and $\nu_{sym}NO_2$, respectively. For Fe^{III}, Cu^{II} and Zn^{II} complexes, the position of these bands is unchanged, *i.e.*, nitro-coordination is not observed. For Mn^{II}, Co^{II} and Ni^{II} complexes, these two bands change as follows:

(a) The first and the second bands appear at 1461 and 1402 cm^{-1} due to $\nu_{asym}NO_2$ and $\nu_{sym}NO_2$, respectively.
(b) The $\delta_{(ONO)}$ mode of vibration appeared at 839 cm^{-1} for both Co^{II} and Ni^{II} complexes, and 836 cm^{-1} for the Mn^{II} complex.
(c) A new band for $\rho_{w(NO_2)}$ appeared at 644, 646 and 641 cm^{-1} for Mn^{II}, Co^{II} and Ni^{II} complexes, respectively.
(d) New ν_{M-NO_2} bands are assigned at 411, 413 and 414 cm^{-1} for Mn^{II}, Co^{II} and Ni^{II} complexes, respectively. The presence of the bands ν_{asymNO_2} and ν_{symNO_2}, $\delta_{(ONO)}$, $\rho_{w(NO_2)}$ and ν_{M-N} for Mn^{II}, Co^{II} and Ni^{II} complexes suggested that the nitro group was involved in bonding of the complexes through nitrogen; this was confirmed

by the presence of wagging modes near 620 cm^{-1}. These complexes are classified into two categories: (1) nitro-metal bonding and (2) metal-pyrimidine interaction.

(i) The manganese complex ($MnL_2 \cdot 6H_2O$) exists in a structural configuration where two molecules of the ligand are bidentate. The six water molecules are distributed where two are in the inner sphere (bonded to manganese to satisfy geometry) and the remaining four molecules are in the outer sphere.
(ii) For the iron complex ($FeL \cdot Cl_2 \cdot 3H_2O$), the ligand is bidentate with chelation through nitrogen of the pyrimidine ring and —OH of the enol form. The two water molecules in the inner sphere are directly attached to iron while the third water molecule is in the outer sphere.
(iii) The cobalt complex ($CoL_3 \cdot 2H_2O$) exists in a structure where the molecules of the ligand are bidentate through the nitrogen of the nitro group and oxygen of the —OH group, formed by tautomerism. The two water molecules are in the outer sphere.
(iv) The nickel complex ($NiL_3 \cdot 5H_2O$) exists in a similar configuration to the cobalt complex, where five water molecules in the former complex are outer sphere.
(v) The copper complex ($CuL_2 \cdot H_2O$) exists in a geometry where the ligands are bidentate with chelation where the pyrimidine nucleus is tautomerized with bonding between the metal and both nitrogen and oxygen atoms of this ring. The water molecule is in the outer sphere.

Electronic Spectra and Magnetic Properties

The magnetic moment values μ_{eff} at room temperature and the nujol electronic absorptions are given in Table I. The $MnL_2 \cdot 6H_2O$ complex gave five bands at 40820, 33840, 31100, 27917 and 17920 cm^{-1} and room temperature $\mu_{eff} = 5.88$ B.M. The first three bands are due to the effect of the metal ion on the $\pi \rightarrow \pi^*$ electronic transitions of the free ligands. The fourth and fifth bands are identified to the complex itself with d–d electronic transitions. The bands at 27917 and 17920 cm^{-1} are assigned to the octahedral geometry [65, 66]. The iron complex gave four bands at 38869, 28469, 21276 and 16120 cm^{-1}. The first two bands are due to the effect of the metal ion on the $\pi \rightarrow \pi^*$ electronic transitions of the free ligand. The broad bands at 21276 and 16130 cm^{-1} are typical for octahedral completes.

Such data with the room temperature magnetic moment $\mu_{eff} = 6.1$ B.M. suggest an octahedral high spin configuration. The $[CoL_3 \cdot 2H_2O]$ complex gave charge transfer bands at 42800 and 33222 cm^{-1}. The visible $d-d$ electronic spectral band at 20000 cm^{-1} assigned to the transition $^4T_{1g}(F) \rightarrow ^4T_{1g}(P)$ of an octahedral cobalt complex [67] and the measured magnetic moment value (Tab. I) are typical of octahedral high spin [68]. The bluish green nickel complex $(NiL_3 \cdot 5H_2O)$ gave four bands at 41666, 31305, 25000 and 18050 cm^{-1} the first two bands are due to the nickel (II) effect on the $\pi \rightarrow \pi^*$ electronic transitions of the free ligand. The last two bands are assigned to octahedral spin-allowed $^3A_{2g} \rightarrow ^3T_{1g}(F)$ and $^3A_{2g} \rightarrow ^3T_{1g}(P)$ transitions, respectively. The room temperature effective magnetic moment value of 3.4 B.M. reflects spin-orbit coupling in the octahedral configuration. The pale green $[CuL_3 \cdot H_2O]$ complex gave three bands at 40650, 31250 and 18870 cm^{-1} and $\mu_{eff} = 2.3$ B.M. The first two bands are due to the effect of the metal ion on the $\pi \rightarrow \pi^*$ electronic transitions of the free ligand the third band is due to the complex itself. All data indicate octahedral configuration. The proposed structures of the complexes are shown in Figure 3.

Studies on Mixed-metal Complexes

Two samples of mixed metal (Fe–Co and Fe–Ni) complexes of 5-nitrobarbituric acid compound were prepared. The nujol mull electronic absorption spectra and room temperature magnetic susceptibility measurements are collected in Table I and compared with the simple complexes. The $Ni_3FeL_7Cl_2 \cdot H_2O$ complex gave two nujol mull electronic spectral bands at 30581 and 17690 cm^{-1} and a room temperature magnetic moment $\mu_{eff} = 5.78$ B.M. However, the $Co_3FeL_7Cl_2 \cdot H_2O$ complex gave two nujol mull electronic spectral bands at 30581 and 1760 cm^{-1} and room temperature magnetic moment value $\mu_{eff} = 9.1$ B.M. From the IR, the ν_{OH} broad band at 3400 cm^{-1} in the free ligand moves to 3444 and 3441 cm^{-1} in iron–cobalt and iron–nickel complexes, respectively. The ν_{OH} bands appeared at 3575 and 3578 cm^{-1} for iron–cobalt and iron–nickel complexes, respectively. The $\nu_{C=N}$ bands appeared at 1691, 1657 and 1615 cm^{-1} for iron–cobalt and iron–nickel complexes, (free ligand at 1639 cm^{-1}) suggest the nitrogen atom of the pyrimidine ring formed by tautomerism is bonded to the metal in both of the mixed-metal complexes. The ν_{asymNO_2} and ν_{symNO_2} stretching modes of vibrations appeared at 1464 and 1404 cm^{-1} in the iron–cobalt complex and at 1463 and 1404 cm^{-1} in the iron–nickel complex compared to 1480 and 1383 cm^{-1} in the free ligand

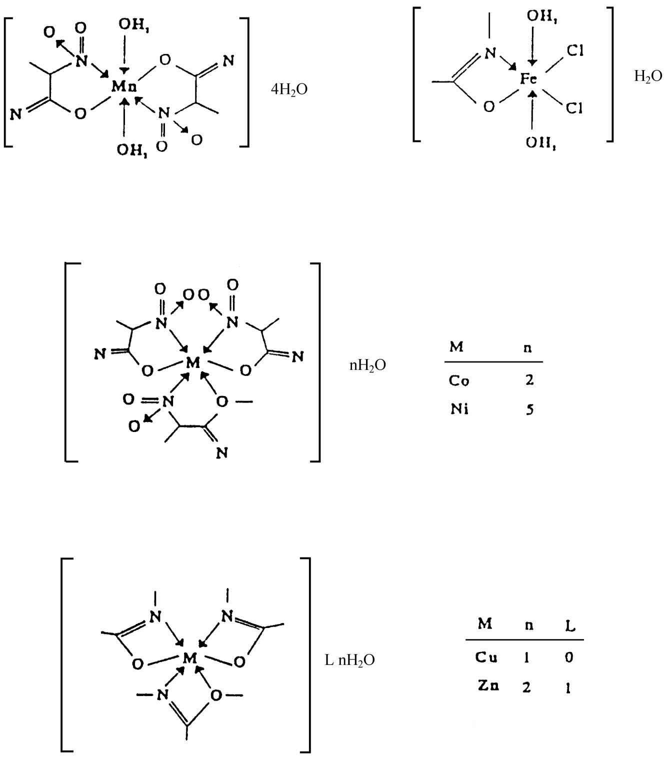

FIGURE 3 Proposed structures of the mono-metallic complexes.

indicating, the nitrogen atom of the —NO_2 group is bonded to the metal. In the simple iron complex, the ν_{asymNO_2} and ν_{symNO_2} bands are not affected on complexation indicating the nitro group is not involved in chelation while in the mixed complexes of iron–cobalt and iron–nickel, the stretching vibration band of the —NO_2 group is affected to give a good criterion for mixed complex formation. This is supported by the presence of $\delta_{(ONO)}$, $\rho_{w(NO_2)}$ and ν_{M-NO_2} at 841, 644 and 412 cm^{-1} in the iron–cobalt complex and at 841, 642 and 417 cm^{-1} in the iron–nickel complex. The presence of wagging modes of vibration near 620 cm^{-1} for both iron–cobalt and iron–nickel mixed complexes confirm the —NO_2 group is bonded to the metal through nitrogen rather than oxygen. The $Ni_3FeL_2Cl_2 \cdot H_2O$ and $Co_3FeL_7 \cdot H_2O$ complexes exist in structures where two molecules of the ligands are bidentate directly to iron through nitrogen of the —NO_2 group and the —OH group formed by tautomerism and with the water molecule directly attached to iron. The reasonable configuration of the iron moiety of the mixed complexes is octahedral with $\mu_{eff} = 5.78$ B.M. However, the nickel is square planar and the cobalt is tetrahedral. The structure of the prepared mixed complexes is suggested as follows:

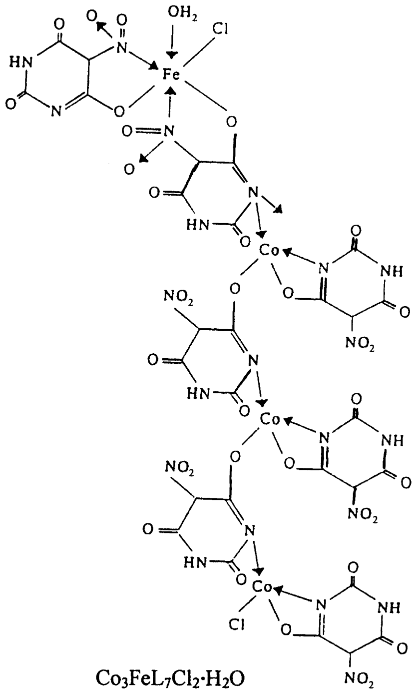

$Co_3FeL_7Cl_2{\cdot}H_2O$

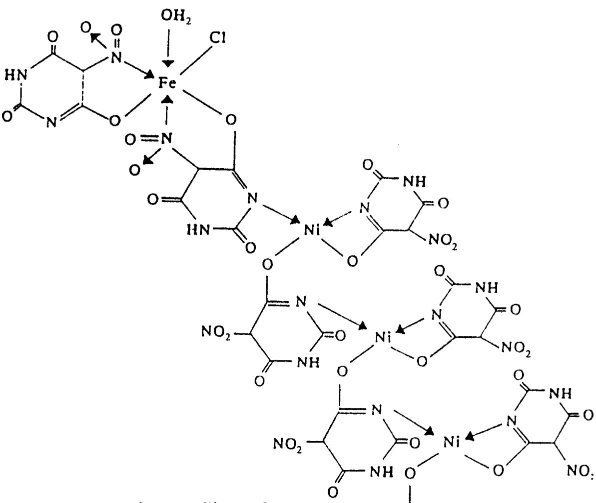

$Ni_3FeL_7Cl_2{\cdot}H_2O$

Mössbauer Spectroscopy

The iron complex gave two peaks, each a doublet indicating the presence of iron in two-oxidation states +2, +3 in l.s. and h.s. states, respectively [69], Figure 4. The isomer shift values, δ(0.136 and 0.660 mm/sec, respectively,

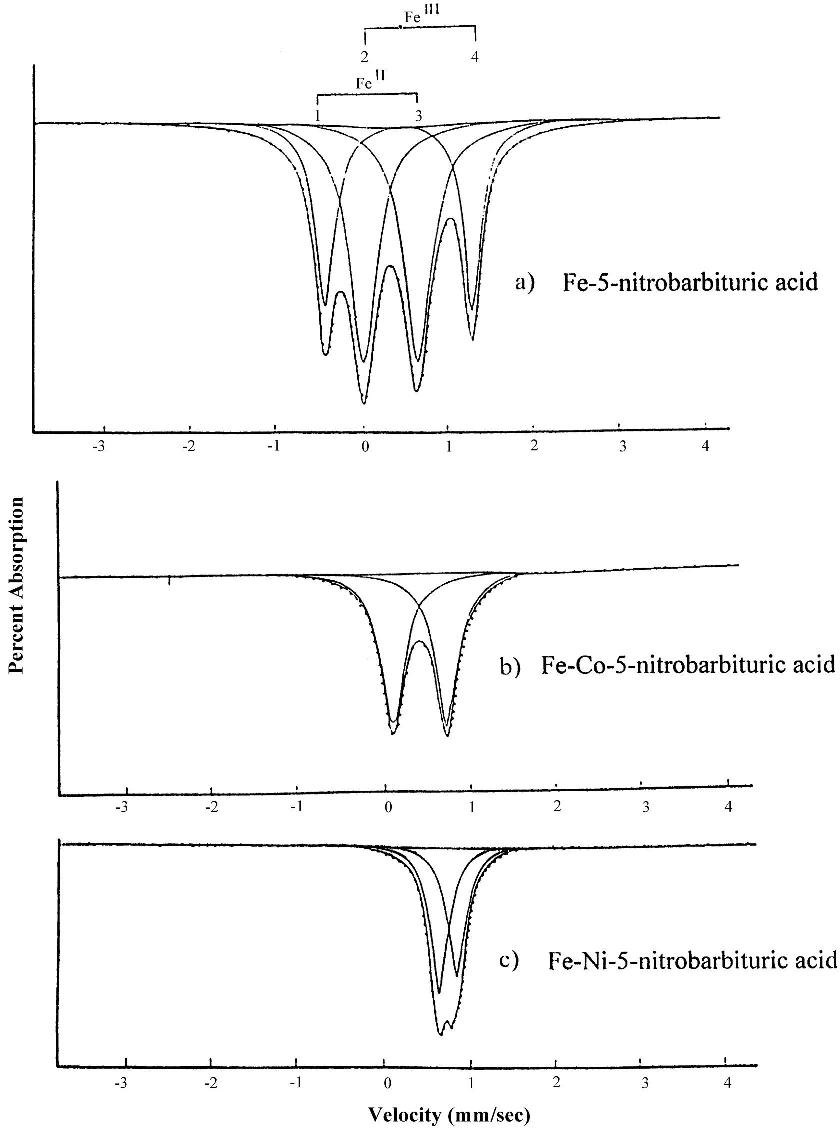

FIGURE 4 Mössbauer Spectra of: (a) Fe-5-nitrobarbituric acid complex. (b) Fe–Co-5-nitrobarbituric acid complex. (c) Fe–Ni-5-nitrobarbituric acid complex.

Table V, where the values of the Fe^{III} lie within those published [69], while that of the Fe^{II} is slightly higher than that known support this assignment [69]. Therefore, both Fe^{II} and Fe^{III} are cooperative within the structure of the complex compound. On the other hand, the ΔE_Q values mm/see, for the Fe^{II} and Fe^{III} are nearly equal (1.233 and 1.031, respectively, Table V. The equal contribution of Fe^{II} and Fe^{III} is established, Table VI. Both complexes are with δ values 0.409 and 0.713 mms^{-1} in case of M=Co and Ni, respectively, meanwhile with ΔE_Q values 0.590 and 0.192, respectively, Table V. Both Co^{II} and Ni^{II} affect the Mössbauer pattern of the iron complex, due to many factors, *e.g.*, oxidation state of the element, geometry, forces of interaction and also molecular formula. This signifies an increase in the local exchange and the spin density. There was an increase in the isomer shift (δ) for the iron–nickel complex and a decrease in the value for the iron–cobalt complex and also a large reduction of the quadrupole splitting (ΔE_Q) in the iron–cobalt and iron–nickel complexes when compared with the iron precursors. The higher value of (δ) in the iron–nickel complex reflects an increase of the *d*-electron screening of the *s*-electrons of the iron nucleus in the iron–nickel complex relative to the iron precursors. Such an increase may have been a result of reduced

TABLE V Mössbauer parameters for structural chemistry of iron, iron–cobalt and iron–nickel complexes of 5-nitrobarbituric acid

Complex	$\delta(mm \cdot s^{-1})$	$\Delta E_Q(mm \cdot s^{-1})$
$FeLCl_2 \cdot 3H_2O$	Fe^{III} 0.660	1.233
	Fe^{II} 0.136	1.031
$Co_3FeL_7Cl_2 \cdot H_2O$	Fe^{III} 0.409	0.590
$Ni_3FeL_7Cl_2 \cdot H_2O$	Fe^{III} 0.713	0.192

TABLE VI Fe^{II}/Fe^{III} ratio of iron-5-nitrobarbituric acid

Peak number	*Half width* $(mm \cdot s^{-1})$	*Height** (*relative counts*)	*Area***	*Iron state*	Fe^{II}/Fe^{III}***
1	8.928	1732.643	15469.037	Fe^{II}	
2	12.444	2260.960	28132.026	Fe^{III}	
					1.033
3	12.874	2241.041	28851.162	Fe^{II}	
4	8.248	1790.690	14769.611	Fe^{III}	

* Number of resonance absorption with respect to the base line (zero absorption).
** Area of the peak = half width × height.
*** Fe^{II}/Fe^{III} is denoted by the ratio of the total area of Fe^{II} divided by the total area of Fe^{III}.

π-back-donation [70]. Isomer shift values vary directly with the *s* orbital character of the iron atom, as well as indirectly with the electronegativities of the ligands attached to it [71]. The low δ value of the iron 5-nitrobarbituric acid complex and for both the Fe–Ni and Fe–Co mixed complexes indicates six-coordinate iron [71]. However, the small ΔE_Q values for Fe–Co and Fe–Ni mixed complexes indicated a near-octahedral configuration around the iron site in the bimetallic complexes [70]. The spectral pattern exhibited an apparent double peak of asymmetry, where the high-energy side of the peak is somewhat broader than the low-energy side. This asymmetry indicates that the absorption line consists of an unresolved quadrupole doublet. This Mössbauer behavior can be understood in terms of the low spin relaxation (fluctuation) process of paramagnetic ions [72]. Paramagnetic fluctuations are caused by spin–lattice and spin–spin interactions. The gradual broadening of the spectrum is attributable to the decreasing effect of spin–lattice interaction [73].

DTA Analysis

All the complexes showed six peaks except for the cobalt and nickel complexes which showed seven and eight peaks, respectively, Figure 5. The DTA curve of the $[ZnL_4 \cdot 2H_2O]$ complex showed a well-defined strong endothermic peak at 140°C and five exothermic peaks at 100.0, 257.6, 268.5, 392.4 and 500°C. The first two peaks are assigned to the dehydration of the outer-sphere water. The peaks at 257.6 and 268.2°C are probably due to the thermal agitation and the decomposition of the fourth ligand in the outer sphere, respectively. However, the last two peaks arrest the composition of $Zn(OH)_2$, which decomposed to ZnO as a final decomposition product. The LnΔT *vs.* 1000/T plots give best fit straight lines for all peaks except for the two dehydration peaks. Each peak gives two straight lines intersecting with each other at a characteristic transition temperature (66 and 117°C). The octahedral $[MnL_2(H_2O)_2] \cdot 4H_2O$ and $[CuL_3] \cdot H_2O$ complexes showed one and two endo-peaks at 157.8°C for the manganese complex and at 117.3, 188.2°C, respectively. The other peaks are exothermic. The peak at 77.9°C in the copper complex is due to a crystallization property while the peak at 117.3°C for the copper complex and those at 98 and 157.8°C for the manganese complex are probably due to dehydration of water adsorbed on the surface of the complexes. The 250°C peak for the Mn^{II} complex is due to dehydration of the coordinated water. The peaks at 188.2, 272 and 280.4°C for copper and manganese complexes, respectively, are probably due to

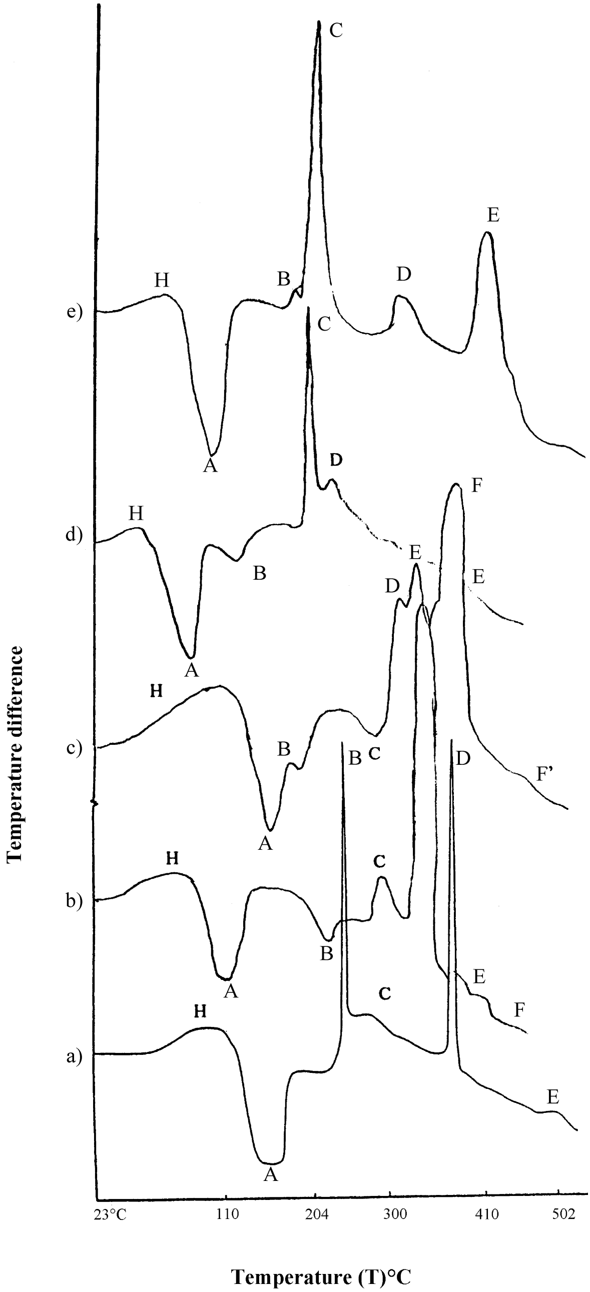

FIGURE 5 DTA curves of 5-nitrobarbituric acid complexes: (a) $[MnL_2(H_2O)_2]\cdot 4H_2O$; (b) $[CoL_3]\cdot 2H_2O$; (c) $[NiL_3]\cdot 5H_2O$; (d) $[CuL_2]\cdot H_2O$; (e) $[ZnL_4]\cdot 2H_2O$.

thermal agitation. The other peaks arrest the material decomposition with the formation of MnO_2 and CO_2 as final products. The octahedral $[CoL_3]\cdot 2H_2O$ and $[NiL_3]\cdot 5H_2O$ complexes gave seven and eight peaks, respectively. The first two peaks at 92.6 and 131.6°C for the cobalt complex and 85.5 and 151.0°C for the nickel complex are due to dehydration of the outer sphere water molecules. The 270°C peak for the cobalt complex and both at 181.3, 287.7°C for the nickel complex may be due to the thermal agitation. The other peaks are due to the material decomposition with formation of Co_2O_3 for the cobalt complex and NiO, NO_2 for the nickel complex as final products. The LnΔT *vs.* 1000/T plots gave straight lines for all the peaks except the first dehydration peaks for the Co^{II}, Ni^{II} and Cu^{II} complexes and the two dehydration peaks in the Mn^{II} complex which give two straight lines intersecting each other at characteristic transition temperatures (69 and 137°C). A representative plot of $\mathrm{Ln}\Delta T - 1000/T$ relation is given in Figure 6. The activation energies and the order of reaction are calculated, Table VII. The data allow the following observations and conclusions:

(1) The first peaks are assigned to dehydration processes to favor the hygroscopic nature for these compounds.
(2) The activation energy of the second dehydration peak for the zinc complex is higher than that of the other complexes. In addition, the energy of activation for the final decomposition step forming ZnO is higher than that of the other complexes.
(3) The zinc complex is of high stability and needs more energy for decomposition than the other complexes due to the electronic configuration and chemistry of zinc.
(4) Despite Mn^{II}, Co^{II}, Ni^{II} and Cu^{II} complexes having the same O_h geometry, they decomposed in a different pattern probably due to the variation in both the chemistry of the transition metal and the stoichiometry of these complexes (Tab. I).
(5) The appearance of fractional orders suggests that the reaction proceeds *via* complicated mechanisms.

The values of the collision factor, Z, were calculated based on the following relation [74]:

$$Z = \frac{\Delta E_a}{RT_m}\varphi \exp.\left(\frac{\Delta E_a}{RT_{m^2}}\right) = \frac{KT_m}{h}\exp.\left(\frac{\Delta S^*}{R}\right)$$

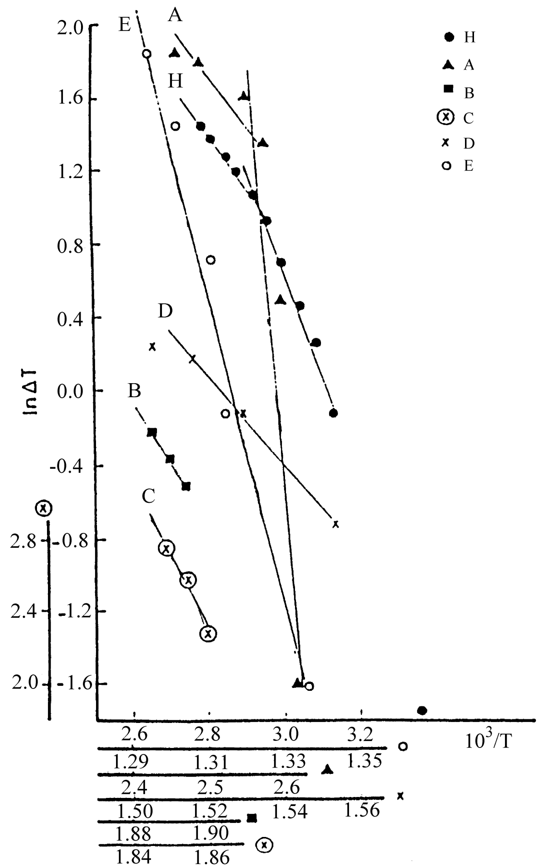

FIGURE 6 $Ln\Delta T - 1000/T$ relation for zinc complexes of 5-nitrobarbituric acid complexes, $[ZnL_4] \cdot 2H_2O$.

where, R represents the molar gas constant, φ is the rate of heating ($°KS^{-1}$), ΔS^* is the entropy of activation, K and h are the Boltzman and Planck's constants, respectively. The change of entropy, ΔS^* values for all complexes, Table VII, are of the same magnitude within the range (-0.220 to $-0.26\,kJK^{-1}\,mol^{-1}$). So, the transition states are more ordered, *i.e.*, in a less random molecular configuration than the reacting complexes. The calculated values of the collision number, Z, showed a direct relation to E_a. The position of the peak is defined by the peak temperature T_m at which the peak maximum or minimum occurs. The values of the decomposed substance fraction, α_m, at maximum development of the reaction was calculated and lies within the range $0.490-0.736$.

TABLE VII Thermal properties of 5-nitrobarbituric acid complexes

T_m °K	n	ΔE_a $kJmol^{-1}$	S	α_m	ΔZ Sec^{-1}	ΔS^* $kJmol^{-1}$	ΔH^* $kJK^{-1}mol^{-1}$	*Comments*	*Assignment*
Mn^{II} complex									
371.0	0.71	71.26	0.314	0.69	4.10	−0.24	−87.19	Before intersection	Loss of outer sphere water molecules
		19.19			1.06	−0.25	−91.27	After intersection	
430.8	0.89	124.71	0.50	0.65	6.29	−0.23	−100.38	Before intersection	Loss of outer sphere water molecules
		3.33			0.16	−0.26	−113.30	After intersection	
553.4	1.71	290.99	1.83	0.53	11.81	−0.23	−127.28	–	Thermal agitation
653.0	Sharp	–	–	–	–	–	–	–	Material decomposition of the complex
765.8	0.94	486.96	0.56	0.64	14.09	−0.23	−176.90	–	Formation of MnO_2
Co^{II} complex									
365.6	0.81	93.12	0.410	0.67	5.55	−0.23	−84.82	Before intersection	Loss of outer sphere water molecules
					1.69				
		29.93				−0.24	−88.48	After intersection	
404.6	1.15	154.39	0.83	0.61	8.57	−0.23	−93.06	–	Loss of outer sphere water molecules
543.0	0.86	246.68	0.46	0.66	10.08	−0.23	125.43	–	Thermal agitation
610.0	2.11	58.20	2.80	0.49	1.95	−0.25	−149.45	–	Material decomposition of the complex
637.8	1.17	49.88	0.86	0.60	1.59	−0.25	−157.54		
673.2	1.21	230.95	0.92	0.58	7.31	−0.24	−158.20		
714.01	1.00	2.5.08	0.63	0.64	6.04	−0.24	−169.22	–	Formation of Co_2O_3
Ni^{II} complex									
358.5	0.93	82.10	0.55	0.65	4.96	−0.23	−83.53	Before intersection	Loss of outer sphere water molecules
		18.07			1.03	−0.25	−88.19	After intersection	
424.0	1.01	90.12	0.64	0.63	4.52	−0.24	−99.64	–	Loss of outer sphere water molecules

454.3	1.13	276.86	0.80	0.61	14.35	−0.23	−102.67	–	Thermal agitation
560.7	0.80	199.54	0.40	0.67	7.70	−0.23	−130.64		
581.0	1.31	137.18	1.08	0.58	4.97	−0.24	−137.70	–	Material decomposition of the complex
604.4	1.35	831.4	1.14	0.58	36.27	−0.22	−133.57		
651.2	1.19	72.30	0.89	0.60	2.27	−0.25	−159.26		
749.5	0.55	157.97	0.19	0.74	4.37	−0.24	−179.88	–	Formation of NiO and NO_2
Cu^{II} complex									
350.9	0.76	58.20	0.37	0.68	3.52	−0.24	−82.81	Before intersection	Loss of outer sphere water molecules
		21.62			1.26	−0.24	−85.62	After intersection	
390.3	0.94	73.66	0.55	0.64	4.01	−0.24	−92.11	–	Loss of outer sphere water molecules
461.2	0.81	37.41	0.41	0.67	1.66	−0.24	−112.53	–	Thermal agitation
576.4	0.97	224.31	0.59	0.64	8.55	−0.23	−134.30	–	Material decomposition of the complex
684.8	1.08	101.85	0.74	0.62	3.06	−0.24	−166.41	–	Formation of CO_2
Zn^{II} complex									
373	0.81	47.47	0.413	0.670	2.66	−0.42	−89.15	Before intersection	Loss of outer sphere water molecules
		24.00			1.37	−0.24	−91.01	After intersection	
413	1.16	415.70	0.846	0.61	27.05	−0.22	−90.86	Before intersection	Loss of outer sphere water molecules
		47.51			2.39	−0.24	−99.12	After intersection	
530.6	1.09	290.99	1.333	0.62	12.45	−0.23	−121.51	–	Decomposition of ligand outer sphere molecule
541.2	1.26	332.56	1.00	0.59	14.13	−0.23	−123.39	–	Thermal agitation
665.4	1.20	195.63	0.91	0.60	6.12	−0.24	−157.03	–	Material decomposition of the complex
773	1.36	715.00	1.17	0.57	21.41	−0.23	−175.47	–	Formation of ZnO

References

[1] W. C. Cutting, *Handbook of Pharmacol.* 1.99.3rd edn., Meredith Publishing Company, New York (1967).
[2] A. N. Kharchuk, G. V. Protopoova, V. G. Telyuk, K. V. Fedotov and E. K. Milkitenko, *Fiziol. Akt. Veshchestva* **20**, 21 (1988); C.A. 109.208146 d (1988).
[3] R. G. Sans and M. G. Chozas, *Pharmazie* **43**(12), 827 (1988); CA. 110.146971d (1989).
[4] M. S. Masoud, A. M. Heiba and F. M. Ashmawy, *Trans. Met. Chem.* **8**, 124 (1983).
[5] M. S. Masoud, A. A. Hasanien and A. M. Heiba, *Spectroscopy Lett.* **17**(8), 441 (1984).
[6] M. S. Masoud and A. M. Heiba, *Current Science* **54**(2), 1165 (1985).
[7] M. S. Masoud, N. A. Ibrahim, S. A. Abou Ali, G. Y. Ali and I. M. Abed, *Ind. J. Chem.* **25A**, 389 (1986).
[8] M. S. Masoud, E. A. Khalil and M. E. Kassem, *Reactivity of Solids* **2**, 269 (1986).
[9] A. A. Hasanein, M. S. Masoud and A. M. Heiba, *The Indian Textile Journal* **3**, 110 (1987).
[10] M. S. Masoud, S. A. Abou Ali, G. Y. Ali and I. M. Abed, *Thermochim. Acta* **122**, 209 (1987).
[11] A. A. Hasanein, M. S. Masoud and A. M. Heiba, *J. Chem. Soc. Pak.* **9**(2), 199 (1987).
[12] M. A. El-Dissouky, M. S. Masoud, F. Ali and S. Abou El-Enein, *Affinidad* **416**, 321 (1988).
[13] M. S. Masoud, E. M. Soliman, A. E. El-Kholy and E. A. Khalil, *Thermochim. Acta* **136**, 1 (1988).
[14] M. S. Masoud and Z. M. Zaki, *Trans. Met. Chem.* **13**, 321 (1988).
[15] M. S. Masoud, E. M. Soliman and A. M. Heiba, *Trans. Met. Chem.* **14**, 175 (1989).
[16] M. S. Masoud and Z. M. Zaki, *Bull. Fac. Sci., Mansoura Univ.* **17**, 71 (1990).
[17] M. S. Masoud, M. A. El-Dessouky, F. A. Aly and S. A. Abou El-Enein, *Trans. Met. Chem.* **15**, 443 (1990).
[18] M. S. Masoud, E. A. Khalil and A. R. Youssef, *Synth. React. Inorg. and Met.-Org. Chem.* **20**, 793 (1990).
[19] M. S. Masoud, S. S. Haggag, E. M. Soliman and M. El-Shabasy, *J. of Material Science* **26**, 1109 (1990).
[20] M. S. Masoud, S. A. Abou El-Enein and E. El-Shereafy, *J. of Thermal Analysis* **37**, 365 (1991).
[21] M. S. Masoud and E. A. Khalil, *Polish J. Chem.* **65**, 933 (1991).
[22] M. S. Masoud, M. E. Kassem, Y. Abd El-Aziz and S. M. Khalil, *Bull. Fac. Sci. Mansoura Univ.* **18**, 105 (1991).
[23] M. S. Masoud and S. S. Haggag, *Thermochim. Acta* **196**, 221 (1992).
[24] M. S. Masoud, E. A. Khalil and S. S. Haggag, *Pak. J. Sci. Ind. Res.* **35**, 480 (1992).
[25] M. S. Masoud, S. A. Abou El-Enein and O. F. Hafez, *J. of Thermal Analysis* **38**, 1365 (1992).
[26] M. S. Masoud, M. M. El-Essawi and A. M. Amr, *Anal. Proc.* **29**, 370 (1992).
[27] M. S. Masoud, E. El-Sherealy, E. A. Khalil and O. H. Abd El-Hamid, *Egypt J. Anal. Chem.* **2**, 95 (1993).
[28] M. S. Masoud, S. S. Haggag, H. M. El-Nahas and N. Abd El-Hi, *Acta Chim. Hung.* **130**, 783 (1993).
[29] E. A. Khalil, M. S. Masoud and A. El-Marghany, *Pak. J. Sci. Ind. Res.* **36**, 68 (1993).
[30] M. S. Masoud, Z. M. Zaki, F. M. Ismail and A. K. Mohamed, *Z. Fur. Phys. Chem. (N.F.)* **185**(S), 223 (1994).
[31] M. S. Masoud, O. H. A. El-Hamid and Z. M. Zaki, *Trans. Met. Chem.* **19**, 21 (1994).
[32] M. S. Masoud, S. S. Haggag, Z. M. Zaki and M. El-Shabasy, *Spectroscopy Lett.* **27**, 775 (1994).
[33] M. S. Masoud, A. El-Khatib and S. Abd El-Aziz, *Alexandria Engineering J.* **33**, D103, (1994).
[34] M. S. Masoud, O. F. Hafez and N. A. Obeid, *Pak. J. Sci., Ind. Res.* **37**, 421 (1994).
[35] M. S. Masoud, H. M. El-Nahas and S. S. Haggag, *Pak. J. Sci. Ind. Res.* **38**, 108 (1998).
[36] M. S. Masoud, S. S. Haggag and O. H. Abd El-Hamid, *Revue Roumain De Chimie* **41**, 21 (1996).
[37] M. S. Masoud, M. M. Ghonaim and O. Heiba, *Egypt J. Appl. Sci.* **11**, 302 (1996).

[38] M. S. Masoud, A. A. Hasanein, A. K. Ghonaim, E. A. Khalil and A. A. Mahmoud, *Z. Fur. Phys. Chem.* **209**, S. 223 (1999).
[39] M. S. Masoud, A. M. Hindawy and R. H. Ahmed, *Pak. J. Sci. Ind. Res.* **42**(1), 11 (1999).
[40] M. S. Masoud, E. A. Khalil, A. A. Ibrahim and A. A. Marghany, *Z. Fur. Phys. Chem.* **211**, 13 (1999).
[41] M. S. Masoud and H. H. Hammud, *Ultra Scientist for Physical Sciences* **12**, 12 (2000).
[42] M. S. Masoud, S. A. Abou El-Enein and H. M. Kamel, *Ind. J. Chem.* accepted for Publication (2001).
[43] M. S. Masoud, A. Kh. Ghonaim, R. H. Ahmed, A. A. Mahmoud and A. E. Ali, accepted for publication, *Z. Fur. Phys. Chem.* (2000).
[44] M. S. Masoud, S. A. Abou El-Enein and N. A. Obeid, accepted for publication, *Z. Fur. Phys. Chem.* (2000).
[45] O. N. Yalcindag, *J. Pharm. Belg.* **38**(6), 321 (1983); C.A. 100,180181z (1984).
[46] O. N. Yalcindag and Turk Hij, *Deneysel Biyol. Derg.* **41**(2), 215 (1984); C.A. 103,129159h (1985).
[47] O. N. Yalcindag, *Sci. Pharm.* **49**(3), 348 (1981); C.A. 96,40998 v (1982).
[48] F. N. M. Naguib and M. H. Elkouni, *Biochem. Pharmacol.* **38**(9), 1471 (1989); C.A. 111,33117g (1989).
[49] V. M. Sadivskii, V. V. Petrenko and B. P. Zorya, *Zh. Anal. Khim.* **45**(3), 609 (1990); C.A. 112,240611z (1990).
[50] V. M. Sadivskii, V. V. Petrenko, B. P. Zorya, Yu. T. Rotberg and T. S. Barabash, *Larv. Kim. Z.* (2), 240 (1991); C.A. 115,79026 n (1991).
[51] V. M. Sadivskii, B. P. Zorya and V. V. Petrenko, *Orkrytiya. Izobret.* **45**, 177 (1991); C.A. 118,72898 b (1993).
[52] V. M. Sadivskii and V. V. Petrenko, *Farmatsiya* (Moscow) **42**(3), 53 (1993); C.A. 121,141901y (1994).
[53] S. M. Hassan and E. M. Elnemma, *Analyst* **114**, 1033 (1989).
[54] M. A. Ahmed, *Analyst* **119**(6), 1367 (1994).
[55] M. Ponii, M. Bostan, N. Iovags and I. Gase, *Rev-Roum. Chim.* **9**, 572 (1964).
[56] K. E. Daugherty, M. W. Coheem, R. J. Robinson and J. I. Muller, *Anal. Chem.* **36**, 2373 (1964).
[57] V. N. Biryulina, R. A. Chupakhina and V. V. Serebrennikov, *Zh. Obshch. Khim.* **54**, 382 (1984); C.A. 100,150069 b (1984).
[58] L. G. Van Vitert and C. G. Hass, *J. Am. Chem. Soc.* **75**, 451 (1953).
[59] B. N. Figgis and J. Lewis, "*Modern Coordination Chemistry*", Interscience, New York, p. 403 (1967).
[60] H. Irving and H. Rossotti, *J. Chem. Soc.* p. 3397 (1953); p. 2904 (1954).
[61] D. V. Jahagiri and S. B. Rao, *J. Inorg. Nucl. Chem.* **36**, 353 (1974).
[62] S. Charberk and A. E. Martell, *J. Am. Chem. Soc.* **74**, 5052 (1952).
[63] S. Olavi and B. G. Harry, *Inorg. Chem.* **13**, 1185 (1974).
[64] K. K. Mull, W. A. McBryde and Nolboar, *Can. J. Chem.* **52**, 1821 (1974).
[65] S. Olavi and B. G. Harry, *Inorg. Chem.* **13**, 1185 (1974).
[66] C. Paen and G. Tosi, *Aust. J. Chem.* **29**, 543 (1976).
[67] K. Jorgensen, "*Absorption Spectra and Chemical Bonding in Complexes*", Pergamon Press (1962).
[68] B. N. Figgis, "*Introduction to Ligand Fields*", Inter-Science Publication, John Wiley and Sons, New York (1966).
[69] S. I. Lippard and J. M. Berg, "*Principles of Bioinorganic Chemistry*", University Science Books, Mill Valley, California, p. 19 (1994).
[70] M. K. Morigaki, L. C. Machado and C. Larica, *Trans. Met. Chem.* **19**, 599 (1994).
[71] A. G. Davies, P. J. Smith, F. G. A. Stone and E. W. Abel, *Comprehensive Organometallic Chemistry* p. 523 (1982).
[72] J. P. Declereq, J. Feneau-Dupont and Ladriere, *Polyhedron* **14**, 1943 (1995).
[73] S. Iijima, F. Mizutani, M. Mitsumi, N. Matsumoto and H. Okawa, *Inorg. Chim. Acta* **253**, 47 (1996).
[74] H. Horowitz and G. Metzger, *Anal. Chem.* **35**, 1464 (1963).